Desalination and Water Treatment
www.deswater.com

doi: 10.5004/dwt.2023.30054

312 (2023) 14–27
November

Analysis and evaluation of circulated water gap membrane distillation process for water desalination

Suhaib M. Alawad[a], Atia E. Khalifa[a,b,*], Dahiru Lawal[c], Abdul Hafiz Al Hariri[b], Mohamed Antar[b,c], Wail Falath[c,d]

[a]*Interdisciplinary Research Center for Renewable Energy and Power Systems (IRC-REPS), King Fahd University of Petroleum & Minerals, Dhahran, Saudi Arabia, emails: akhalifa@kfupm.edu.sa (A.E. Khalifa), suhaib.ahmed@kfupm.edu.sa (S.M. Alawad)*
[b]*Mechanical Engineering Department, King Fahd University of Petroleum & Minerals, Dhahran, Saudi Arabia, emails: g202110370@kfupm.edu.sa (A.H. Al Hariri), antar@kfupm.edu.sa (M. Antar)*
[c]*Interdisciplinary Research Center for Membranes and Water Security (IRC-MWS), King Fahd University of Petroleum & Minerals, Dhahran, Saudi Arabia, emails: dahiru@kfupm.edu.sa (D. Lawal), wfallata@kfupm.edu.sa (W. Falath)*
[d]*Materials Science and Engineering Department, King Fahd University of Petroleum & Minerals, Dhahran, Saudi Arabia*

Received 16 March 2023; Accepted 30 September 2023

ABSTRACT

Water gap membrane distillation is an effective configuration to improve the productivity of the membrane distillation process. This study provides a comprehensive theoretical analysis of a novel water gap membrane distillation (WGMD) design where the gap water is circulated. Circulating the gap water improves the output flux due to the forced convection characteristics inside the water gap and hence improves mass and heat transfer coefficients. The model outcomes are compared with the experimental findings for validation, and it shows a very good agreement with a maximum deviation of less than 10%. The influences of operational variables on the energy efficiency, output flux, and freshwater cost are presented and compared to the standard WGMD process, without circulated gap, under the same operation conditions. Results reveal that the circulated water gap enhances the output flux by a maximum of 350% and reduces the production cost by a maximum of 32%. Regarding energy efficiency, a slight improvement is obtained when the gap water is circulated at a rate of up to 4 L/min; however, using a higher circulation rate reduces the energy efficiency. Using a multistage system to increase productivity can minimize production costs by roughly 82%.

Keywords: Water gap membrane distillation; Flow circulation in the gap; Theoretical investigation; Performance and cost evaluation; Energy efficiency

1. Introduction

Membrane distillation (MD) is a membrane separation technology that utilizes heat to separate water vapor from a saltwater stream. In the MD system, two separate streams, cold and hot, flow within the coolant and feed channels of the membrane cell (module) [1]. A hydrophobic membrane separates the feed and coolant streams, allowing only vapor to flow through [2]. MD technology has several advantages over conventional desalination technologies, such that the technique operates at low temperatures (50°C–90°C) and low pressures and achieves near-100% salt rejection [3]. However, the low output flux is the main challenge facing the MD technique. The basic module configurations of the MD technique include the direct contact membrane distillation (DCMD), sweeping gas membrane distillation, vacuum membrane distillation, and air gap membrane distillation (AGMD). All module configurations have the same

* Corresponding author.

design as the feed side; however, the cold side is different in each type [4,5].

AGMD is one of the commonly utilized membrane distillation configurations. In the AGMD, a gap is created between the membrane and the cold side; stagnant air fills this gap to minimize energy loss between both hot and cold streams. It is proven that introducing the air gap reduces heat loss; however, it also declines the system's production due to increased mass and heat transport resistance inside the gap [6]. Therefore, researchers employed different methods to address this problem. One of these methods is by using the water gap membrane distillation (WGMD). The module design of the water gap arrangement is similar to that of the air gap; however, in the water gap, the gap is occupied by stagnant clean water, which diminishes the resistance of mass transfer due to the immediate vapor condensation within the gap [7]. WGMD process is also referred to as permeate gap membrane distillation (PGMD) or liquid gap membrane distillation in the literature.

Abu-Zeid [8] examined the effect of the permeate gap region (PGR) on the high diffusion resistance and low productivity caused by the air gap region (AGR) sandwiched between the membrane and condensing surface in AGMD. Two hollow fiber modules (PGMD and AGMD) were constructed, characterized, and compared experimentally. The energy consumption, water productivity, and gained output ratio (GOR) were used to compare the performance. The results indicated that PGR was more effective than AGR at improving the membrane module's performance across all operating parameters investigated.

Khalifa [7] compared the performance of water gap and AGMD methods by using a module that could function in both configurations. The water gap design was found to be more efficient due to the lower resistance to vapor movement and better heat transfer within the gap. The output flux of the WGMD design was higher, with an increase of 91% to 141% compared to the air gap system under the same conditions. The permeate flux reduced as the gap size increased, but the water gap system was less affected by changes in gap size compared to the air gap system. However, due to the different thermal properties of air and water, the WGMD design required more energy than the AGMD.

Cai et al. [9] studied the transport analysis of a material-filled gap MD process using various materials as fillers, such as glass and stainless-steel beads. The results indicated that the properties and structure of the fillers play a significant role in determining the transport behavior of the fillers throughout the membrane distillation processes. The membrane distillation performance depends on the fillers' thermal conductivity and the gap's void volume fraction. Thermally conductive fillers can help increase permeate flux.

Essalhi and Khayet [10] studied two different MD systems, the liquid gap and the air gap, under the same design and test conditions. The liquid gap system was found to have a higher flux than the air gap system, with a difference of 2.2%–6.5%. Francis et al. [11] filled the gap in the air gap MD unit with various materials such as deionized water, sponge, and sand. They stated that an improvement of 200%–800% in flux is obtained when the gap was filled with deionized water and sand at various feed temperatures. They also noted that changing the gap size from 9 to 13 mm improved the permeate flux. Experiments were conducted by Khalifa [12] on a novel design to improve the productivity and energy efficiency of the WGMD system. This design used a separate closed loop to circulate the gap water, which improved the heat and mass transfer. According to the results, gap water circulation increased the output flux by 80%–96% compared to the baseline WGMD design.

Alawad et al. [13] investigated the performance of a new system called propeller-aided water gap membrane distillation (P-WGMD) by utilizing mathematical models to analyze heat and mass transfer. The P-WGMD system includes a rotating propeller blade that enhances heat and mass transfer in the gap space. Results showed that the P-WGMD system outperforms the baseline WGMD system, achieving a maximum flux of 322 kg/m^2·h.

Alawad et al. [14] presented the analysis and optimization of a large-scale multistage water gap membrane distillation (WGMD) unit with an internal gap propeller. A mathematical model is developed and combined with a differential evolution (DE) algorithm to optimize the design variables of the gap and system operating parameters. The optimized results indicated that the parallel arrangement of stages demonstrates higher production of 1,738 L/h and lower freshwater cost of \$1.027/m^3.

Mahmoudi et al. [15] conducted experimental evaluations on a WGMD system with internal heat recovery. Performance was assessed using output flux, specific thermal energy consumption (STEC), and GOR indicators. Under conditions of 82°C feed inlet temperature, 15°C coolant inlet temperature, and 1 L/min feed flow rate, the highest output flux was 10 kg/m^2·h. However, the lowest STEC and highest GOR were achieved at a feed flow rate of 0.1 L/min, measuring 1,000 kWh/m^3 and 0.7, respectively.

This proposed design offers several benefits over the traditional WGMD process [10–13]. Notably, due to the enhanced mixing within the gap, the circulation results in a uniform temperature distribution within the gap. Additionally, water movement increases the overall mass and heat transport coefficients within the MD module, increasing the condensation rate and hence the rate of freshwater production. Comparatively, the circulated WGMD system presents advantages over the well-known DCMD process. Specifically, the cooling process in the circulating water gap is separated from the vapor condensation and collection in the gap. This gives more flexibility in designing and selecting the cooling method and fluid. It allows the collection of freshwater separately and using of untreated cooling water in other heat exchange processes if needed. The existing literature pointed out the attention of researchers towards enhancing the efficiency of the MD process through various new designs and methodologies.

Reviewing the available literature showed that there is only one study that has experimentally investigated the idea of water gap circulation in WGMD process [12], and a detailed theoretical investigation of the circulated WGMD process is not available in literature. Thus, the current study aims to conduct a thorough theoretical analysis on the circulated WGMD process to understand the new complex effects of circulating the water gap on the process productivity and energy consumption. The resulting knowledge and data of this study can be used as a benchmark for

further improvements on the process design and operation for better system's performance and a cost-effective water production. The permeate water inside the gap of a WGMD module is circulated in a separate closed cycle while exchanging heat with the hot feed and coolant streams in the WGMD module. The circulation of the product water in the gap enhances the heat and mass transfer characteristics, and one can control the system's performance by controlling the gap design, dimensions, gap temperature, and the gap water circulation rate.

In this study, the coupled analysis of heat and mass transfers within the circulated WGMD module is performed. To ensure that the theoretical results are accurate, the model is validated against experimental results reported by Khalifa [12]. Following the validation, the model is used to conduct a comprehensive parametric study to understand the effects of water gap circulation on various design and operating parameters and to evaluate their effects on the system performance. The flow rate and temperature of both hot feed and coolant streams, the flow rate of the circulated gap stream, and the thickness of the water gap are investigated. Performance indicators include the calculations of the energy efficiency as manifested by the GOR and the specific energy consumption (SEC), the output flux (productivity), the production cost as a techno-economic analysis tool of evaluation. Additionally, the system's performance is compared to the conventional WGMD design (without gap circulation). The accuracy of the developed model allows investigation of a wide range of operating parameters that are difficult to conduct experimentally. The model is solved using the Engineering-Equation-Solver (EES) software.

2. Model

In this part, the mass and heat transfers inside the MD unit are simulated to determine the rate of distillate obtained, and to evaluate the energy efficiency of the WGMD process with the gap water circulation. The circulation of the gap water results in forced convection being the mode of heat transport within the gap rather than pure conduction or natural convection [22]. Heat is transported from the hot to the cold water within the MD unit in different forms. Fig. 1 depicts the module's internal design and the expected distribution of the temperature across the module which is associated with mass and heat transfer modes throughout the WGMD unit with flow circulation in the gap. For clarity, Fig. 2 represents a schematic of the WGMD cell with the feed, coolant, and flow circulation in the gap loops.

2.1. Heat transfer through the feed channel

Convection transfers heat from the hot water to the membrane surface on the hot side of the MD unit (inside the hot water channel). This heat rate can be estimated in Eq. (1) [16]:

$$Q_f = h_f \times \left(T_{\mathrm{bf}} - T_{\mathrm{mf}}\right) \times A_f \tag{1}$$

The heat transport coefficient in the hot water channel due to convection is symbolized as h_f. The temperatures of the hot water and hot membrane surface are represented by T_{bf} and T_{mf}, respectively. The area of the membrane in contact with the hot water stream is denoted as A_f.

2.2. Heat and mass transport through the membrane

A portion of the heat transferred to the membrane [Eq. (1)] is carried across the membrane via conduction ($Q_{\mathrm{conduction}}$), through the membrane material, as a result of the temperature variation across the membrane, while the remaining part is carried across the membrane via evaporation ($Q_{\mathrm{evaporation}}$). The analysis is based on a polytetrafluoroethylene (PTFE) membrane with pore size of 0.45 μm, porosity of 0.8, contact angle of 140°, liquid entry pressure (LEP) of 2.4 bar, and membrane thickness of 7 μm (the same measured properties of the membrane as reported by Khalifa [12]). It is assumed that the operating flow pressures are well below the LEP and thus there is no chance for membrane wetting.

The total rate of heat transferred across the membrane is calculated as:

$$Q_{\mathrm{membrane}} = Q_{\mathrm{conduction}} + Q_{\mathrm{evaporation}} \tag{2}$$

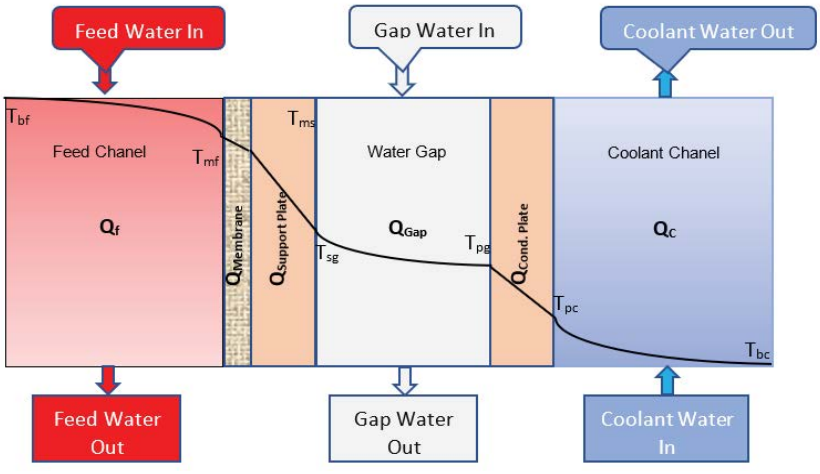

Fig. 1. Temperature distribution across the WGMD module with flow circulation in the gap.

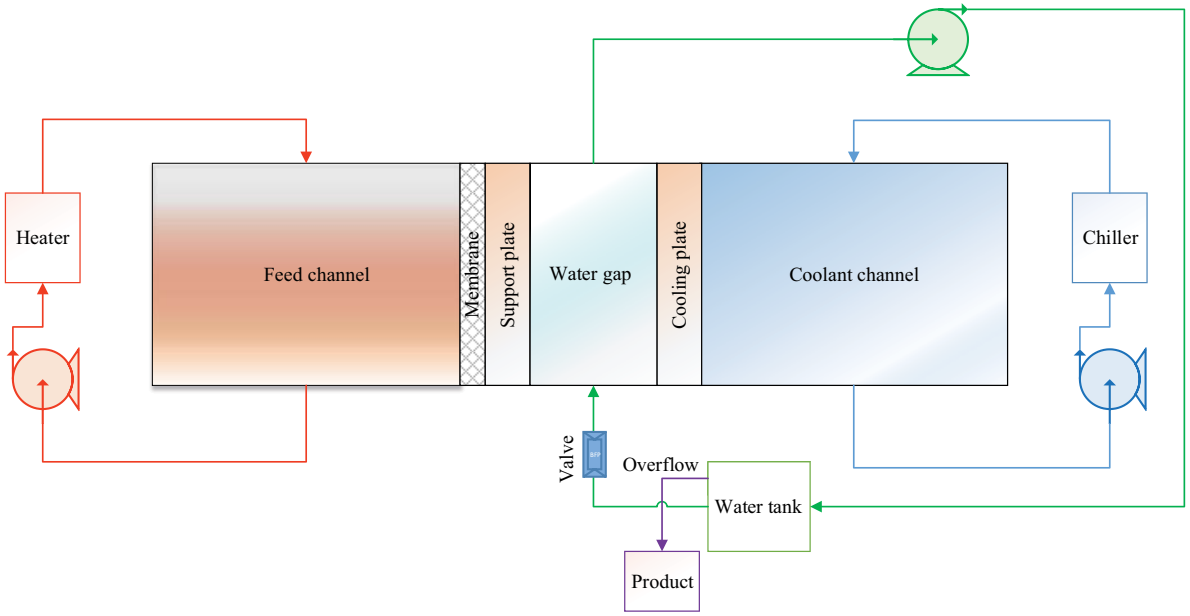

Fig. 2. Schematic of the WGMD module with feed, coolant, and gap water circulation loops.

$$Q_{\text{conduction}} = \left(\frac{k_{m,c}}{\delta}\right) \times \left(T_{\text{mf}} - T_{\text{ms}}\right) \times \text{A}_f \tag{3}$$

$$Q_{\text{evaporation}} = J_w \times \Delta H_v \times \text{A}_v \tag{4}$$

where $k_{m,c}$ is the thermal conductivity of the membrane, δ is the thickness of the membrane, T_{ms} is the temperature at the membrane surface in contact with the support plate, J_w is the mass flow rate of the distillate/freshwater, ΔH_v is the enthalpy of vaporization for the water, A_v is the effective vapor mass transfer area through the membrane.

The temperature variation across the membrane results in a vapor pressure change between the cold and hot sides, which causes water vapor to pass from the hot to the cold side. The rate of water vapor that passes through the membrane is referred to as the permeate flux of the MD process [5,17,18]:

$$J_w = D_e \times \left(P_{\text{mf}} \cdot \gamma_{\text{wf}} \cdot X_{\text{wf}} - P_{\text{ms}}\right) \tag{5}$$

where γ_{wf} is the activity factor and X_{wf} is the water in feed mole fraction [19]. The vapor pressures on the cold side (P_{ms}) and hot side (P_{mf}) of the membrane are mainly functions of temperatures. D_e is the diffusion coefficient.

The activity coefficient can be calculated using Eq. (6):

$$\gamma_{\text{wf}} = 1 - \left(\frac{X_{\text{Nacl}}}{2}\right) - \left(10 \times \left(X_{\text{Nacl}}\right)^2\right) \tag{6}$$

where X_{NaCl} represents the feed concentration. The diffusion coefficient D_e can be calculated as:

$$D_e = \left(\left(\frac{\alpha}{D_k}\right) + \left(\frac{1-\alpha}{D_m}\right)\right)^{-1} \tag{7}$$

where α is the ratio of Knudsen diffusion to molecular diffusion, and it is assumed between 0 and 1 [16] for mixed diffusion mode of vapor through membrane pores. D_m and D_k are the molecular and Knudsen diffusion coefficients. The Knudsen diffusion coefficient D_k is a function of membrane thickness δ, membrane porosity ε, membrane tortuosity τ, pore diameter d_{pore}, seawater molecular weight M_w and average temperature across the membrane T_m. The Knudsen diffusion coefficient is calculated by the Eq. (8) [16]:

$$D_k = \left(\left(\frac{3 \cdot \delta \cdot \tau}{2 \cdot \varepsilon \cdot d_{\text{pore}}}\right) \cdot \left(\frac{\pi \cdot R \cdot T_m}{8 \cdot M_w}\right)^{0.5}\right)^{-1} \tag{8}$$

whereas the molecular diffusion coefficient D_m depends on average temperature across the membrane T_m, membrane thickness δ, membrane porosity ε, membrane tortuosity τ, partial pressure of air inside membrane pores $P_{\text{air,pore}}$, seawater molecular weight M_w and the water vapor diffusion into air molecules $\text{PD}_{w,a}$. The molecular diffusion coefficient can be written by the study of Khayet and Matsuura [16]:

$$D_m = \left(\frac{R \cdot T_m \cdot \delta \cdot \tau \cdot P_{\text{air,pore}}}{M_w \cdot \varepsilon \cdot \text{PD}_{w,a}}\right)^{-1} \tag{9}$$

The vapor pressures can be estimated using Antoine's relation [16]:

$$P_{\text{mf}} = \exp\left(23.1964 - \left(\frac{3816.44}{T_{\text{mf}} - 46.13}\right)\right) \tag{10}$$

$$P_{\text{ms}} = \exp\left(23.1964 - \left(\frac{3816.44}{T_{\text{ms}} - 46.13}\right)\right) \tag{11}$$

2.3. Heat transfer through the support plate

When high flow rates are used on the hot water side, the membrane may bend due to the pressure applied to the membrane by the hot water. When the membrane is deflected, the gap size may change. To avoid membrane deflection, a perforated plate is inserted into the MD unit to support the membrane, allowing the gap thickness to be precisely set and measured.

Conduction across the membrane to the gap through the support plate's perforations, conduction across the plate's solid part, and heat that moves with the vapor as it passes through the supporting plate's perforations are the three different ways that heat can be transferred across the support plate. As a consequence of this, the expression that is provided below can be applied in order to calculate the overall rate of heat transfer across the support plate [19]:

$$Q_{\text{support-plate}} = \frac{k_{\text{support}}}{\delta_{\text{support}}} \times \left(T_{\text{ms}} - T_{\text{sg}}\right) \times \text{A}_{\text{support}} + \frac{k_{m,c}}{\delta} \times \left(T_{\text{mf}} - T_{\text{ms}}\right) \times \text{A}_{v} + \left(J_{w} \times \Delta H_{v}\right) \times \text{A}_{v} \quad (12)$$

The conductivity of the support plate is denoted by k_{support}, while the thickness of the plate is denoted by δ_{support}. T_{sg} is the temperature that is measured on the surface of the support plate that touch the gap water. A_{support} is the closed area on the supporting plate.

2.4. Heat transport in the water gap with gap circulation

For the conventional WGMD process, heat transfers across the gap by mixed conduction and natural convection as discussed and proved by Francis et al. [11], Alawad and Khalifa [19] and Im et al. [20]. However, when the water in the gap is circulated the ratio of natural to forced convection heat transfers inside a gap is approaching zero as defined by the Richardson number, Ri = Gr/Re^2. Ri is a dimensionless number that expresses the ratio of the buoyancy term to the flow shear term. When this ratio is much less than unity, the effect of natural convection (buoyancy) is unimportant, and only forced heat transfer is considered. When Ri is greater than unity, the natural convection dominates. Fig. 3 shows the influence of the gap circulation rate on Richardson number, for different feed temperatures from 60°C to 90°C. In general, Ri_{gap} equals unity and above for gap circulating rates below 1.0 to 1.5 L/min (depending on the hot water temperature). Thus, natural convection should be considered in the heat transfer analysis if the circulation rate is below 1 L/min. Above a gap circulating rate of 1.5 L/min, the value of Ri_{gap} is significantly less than one which indicates dominating mode of forced convection heat transfer.

For convection heat transfer, Newton's law of cooling can be applied to estimate the convection heat transport through the water gap:

$$Q_{\text{gap}} = h_{\text{gap}} \times \left(T_{\text{sg}} - T_{\text{pg}}\right) \times \text{A}_{\text{gap}} \quad (13)$$

where h_{gap} is the coefficient of convective heat transfer in the water gap, which is given by Eq. (14):

$$h_{\text{gap}} = \frac{\text{Nu}_{\text{gap}} \cdot k_{\text{gap}}}{D_{h,\text{gap}}} \quad (14)$$

where $D_{h,\text{gap}}$ is the hydraulic diameter of the gap circulation channel.

Nusselt number in the gap (Nu_{gap}):

- For laminar flow inside the gap (when Reynolds number less than 2,300);

$$\text{Nu}_{\text{gap}} = 1.86 \times \left(\text{Re}_{\text{gap}} \times \text{Pr}_{\text{gap}} \times \frac{D_{h,\text{gap}}}{L}\right)^{0.4} \quad (15)$$

- For turbulent flow inside the gap (when Reynolds number more than 2,300);

$$\text{Nu}_{\text{gap}} = 0.036 \times \left(\text{Re}_{\text{gap}}\right)^{0.96} \left(\text{Pr}_{\text{gap}}\right)^{0.33} \times \left(\frac{D_{h,\text{gap}}}{L}\right)^{0.055} \quad (16)$$

2.5. Heat transfer through the cooling/condensation plate

The thinness of both the support plate and the membrane allows for increased heat transfer from the hot water into the gap, which ultimately results in an increase in temperature for the water contained within the gap. Because of this, the MD unit includes a cooling plate as part of its construction. The cooling surface is a conductive metal plate that is used for cooling the gap, which in turn improves the condensation rate. The temperature of the condensation surface is lowered as a result of the cold water that flows along the backside of the plate. The heat moves from the gap through the material of the cooling surface via conduction, and the rate of heat transport across the cooling surface can be calculated using Eq. (17):

$$Q_{\text{cooling-plate}} = \left(\frac{k_{\text{plate}}}{\delta_{\text{plate}}}\right) \times \left(T_{\text{pg}} - T_{\text{pc}}\right) \times A_{\text{plate}} \quad (17)$$

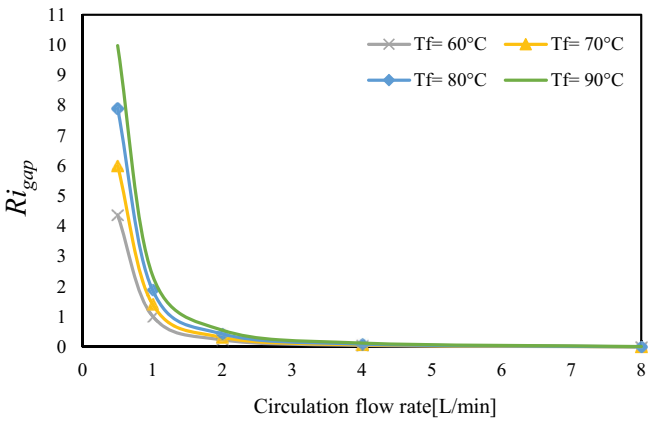

Fig. 3. Richardson number as a function of the circulation rate, at different feed temperatures.

where k_{plate} is the conductivity of the condensation plate material, δ_{plate} is the cooling plate thickness. The temperature measured at the part of the cooling surface that is in contact with the fluid being cooled is denoted by T_{pc}, and the area of heat transport through the condensation plate is denoted by A_{plate}.

2.6. Heat transfer through the coolant channel

Just like in the feeding side, heat is conveyed from the condensation surface to the cold water through convection, and the amount of heat transferred can be calculated using Eq. (18):

$$Q_c = h_c \times \left(T_{pc} - T_{bc}\right) \times A_c \tag{18}$$

The heat transport coefficient in the cold water channel due to convection is symbolized as h_c. The temperature of the cold water is represented by T_{bc}. The area through which the heat is transferred in the cold water channel is denoted as A_c.

In general, the circulated gap MD system can be considered a promising system for freshwater production applications, as it significantly increases the productivity compared to the baseline WGMD module; however, the energy consumption of the new system should be investigated in order to perform a thorough analysis. To assess the energy efficiency of the proposed system, the values of the GOR and SEC are estimated. The GOR measures how much energy is transferred by evaporation in relation to the overall energy used by the MD system. The GOR is calculated using the Eq. (19) [5,21]:

$$\mathrm{GOR} = \frac{J_w \cdot \Delta H_v \cdot A_v}{E_{in}} \tag{19}$$

where E_{in} is the overall power consumed by the MD unit, which is written in Eq. (20):

$$E_{in} = \dot{m}_f \times \mathrm{Cp}_f \times \left(T_{f,in} - T_{f,out}\right) + \dot{m}_c \times \mathrm{Cp}_c \times \left(T_{c,out} - T_{c,in}\right) \tag{20}$$

The mass flow rates of the cold and hot water are represented by $\dot{m}_c$ and $\dot{m}_f$, respectively. The heat capacities of the cold and hot streams are given as Cp_c and Cp_f, respectively. $T_{f,in}$ indicates the feed inlet temperature. $T_{f,out}$ indicates the feed outlet temperature. $T_{c,in}$ represents the coolant inlet temperature. $T_{c,out}$ represents the cold water outlet temperature. The fluids pumping energy is negligible compared to the input thermal energy.

The SEC of an MD unit is represented by the amount of thermal energy needed to make 1 m^3 of pure water (kWh/m^3).

$$\mathrm{SEC} = \frac{E_{in}}{\dot{V}_d} \tag{21}$$

where $\dot{V}_d$ represents the distillate flow rate.

3. Model validation

To ensure that the model outcomes are accurate, results are validated against experimental data reported by Khalifa [12]. Fig. 4 illustrates the comparison of both model and experimental results. The significant parameters influencing the performance of the MD system are used, including hot water flow rate and temperature, cold water flow rate, and a new parameter associated with the new design, which is the circulation rate. The comparison of theoretical and experimental permeate flux at various hot water temperatures is illustrated by Fig. 4a. The comparison is made under operating conditions of 15°C cold water temperature, 5.3 L/min hot water flow rate, 4.3 L/min cold water flow rate, 2.35 L/min circulation flow rate, and 8 mm gap size. The model can accurately predict the permeate flux at various hot water temperatures, with an average calculated difference of approximately 5%. Fig. 4b illustrates the influence of hot water flow rate on output flux in both experimental and theoretical studies. Experiments were conducted at a cold water temperature of 18°C, a hot water temperature of 70°C, 3.5 L/min cold water flow rate, a circulation rate of 2.35 L/min, and a gap size of 8 mm. The model can accurately predict the flux variation as a function of the flow characteristics (laminar or turbulent). It is noticeable that the flux values increase abruptly when the hot water flow rate exceeds 3 L/min; this increase is attributed to the change in the flow from laminar to turbulent with a Reynold value of 2,700 which is greater than the laminar to turbulent transition value of 2,300. The maximum percentage difference between model and lab results is approximately 10%, observed in the transmission region, when the hot water flow rate is around 3 L/min. The change of the output flux with changing the cold water flow rate is carried out for both theoretical and experimental tests under the conditions of 18°C cold water temperature, 8 mm gap size, 3 L/min hot water flow rate, 70°C hot water temperature, and 2.35 L/min circulation flow rate, as shown in Fig. 4c. The model is in excellent agreement with experimental findings, with a maximum error deviation of about 4%. Regarding the new parameter, the circulation flow rate varies from 1.7 to 4.1 L/min while the other parameters remain constant, including the 15°C coolant temperature, the 70°C feed temperature, the 4.3 L/min cold water flow rate, the 5.3 L/min hot water flow rate, and the 8 mm gap size. For all values of the circulation flow rate, the results predicted by the model are quite similar to those observed from experiments, with a maximum difference of about 6% at the low flow rate of 1.7 L/min.

4. Results and discussion

A comprehensive parametric study is conducted to determine the effect of flow circulation in the gap on the performance of the WGMD system. The experimental investigation that was conducted by Khalifa [12] examined the primary operating parameters, including feed inlet temperature, water gap width, coolant inlet temperature, hot and cold water flow rates, and flow circulation in the gap; however, the tested ranges of the operating parameters were constrained by setup capabilities and system operation constraints. For example, the tested feed inlet temperature ranged between 50°C–90°C, the water gap sizes were 8–16 mm, the cold water inlet temperature ranged between 10°C–18°C, the feed flow rate was between 1.3 and 6 L/min,

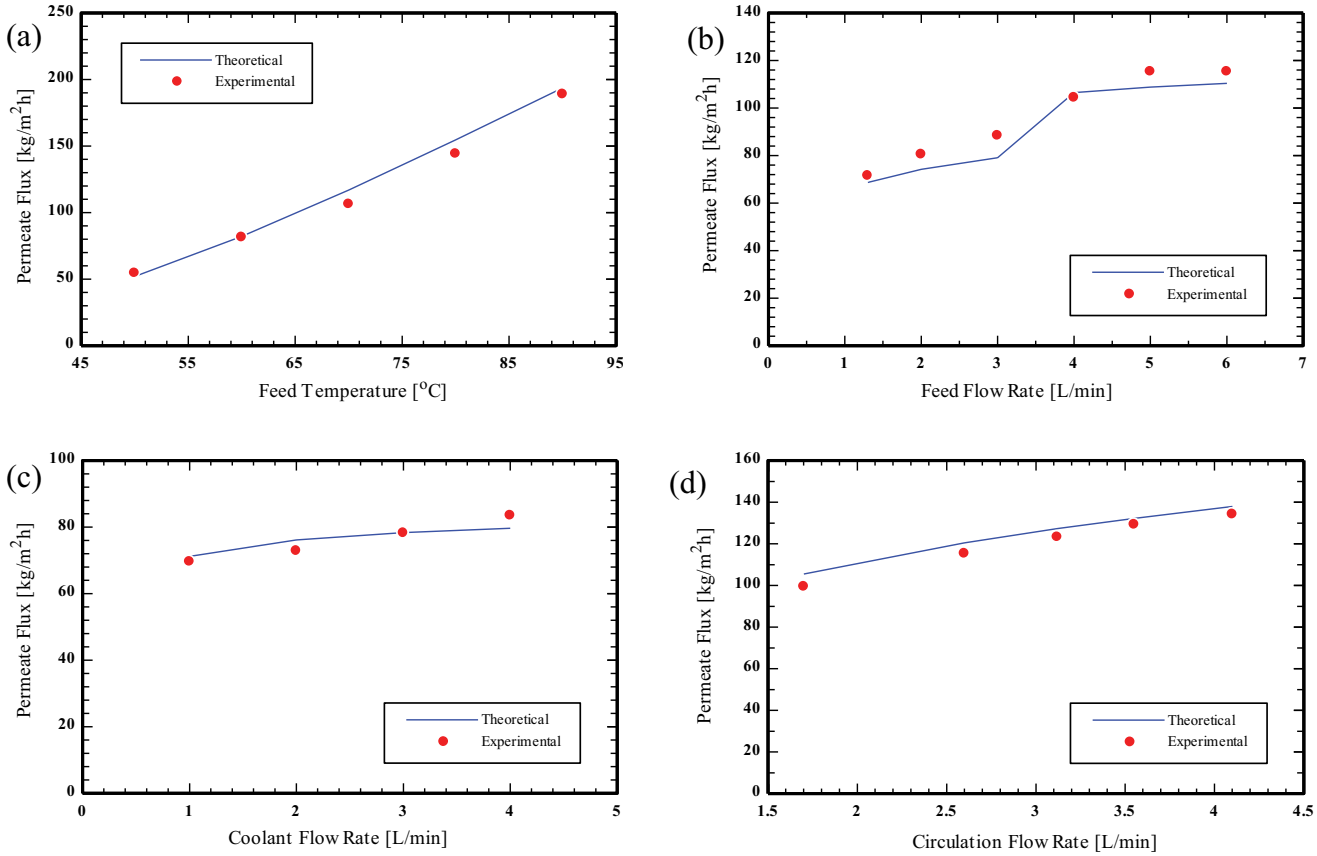

Fig. 4. Model validation at different operating parameters.

the coolant flow rate was between 1 and 4 L/min, and the flow circulation in the gap was between 1.7 and 4.1 L/min. The same operating parameters are examined in this analysis; however, more comprehensive ranges are investigated such that for the same experimental feed temperature range, the coolant temperature increases from 5°C–30°C, the feed, coolant, and circulation flow rates are set from 1–10 L/min, and the gap size is increased from 2–50 mm. The analysis is performed at a constant feed concentration of 150 ppm and a membrane area of 0.0066 m^2. The SEC, production cost, GOR, and output flux are reported and discussed with operating parameters to evaluate the performance of the circulated WGMD unit. The results are then compared to the baseline WGMD module design.

4.1. Effects of operating parameters on the permeate flux

The permeate flux is a commonly used parameter to evaluate the productivity of the MD process. The permeate flux represents the amount of freshwater obtained from the MD system per unit area of the membrane over 1 h. The temperature variation between the cold and hot streams is the driving force for vapor permeation across the membrane. As a result, it is critical to investigate the effects of coolant and feed temperatures on the water production of the WGMD system with circulated gap. Fig. 5a compares the WGMD system with circulated gap to the conventional WGMD system (water gap without circulation) in terms of permeate flux at various hot water temperatures, varying from 50°C to 90°C and different circulation flow rates. Other operating parameters are kept constant, including the coolant temperature of 15°C, the feed and coolant flow rates of 3 L/min, and gap size of 8 mm. As illustrated in Fig. 3a, permeate flux increases as feed temperature increases, for both systems, due to significant growth in the net vapor pressure across the membrane, resulting in a higher distillate production rate. When the hot water temperature changes from 50°C to 90°C, the output flux improves by an average of approximately 270%; however, the system without circulation exhibits a nearly 350% increase in permeate flux under the same conditions. It is easy to see from these high percentages how essential is the feed temperature in the membrane distillation process. It is also discovered that boosting the gap flow rate improves output flux due to the improvement of the gap's heat transfer coefficient associated with the water movement, resulting in an increased condensation rate. At a circulation flow rate of 8 L/min the flow characteristic inside the gap changes from laminar to turbulent for all feed temperatures (all values of Reynolds number within the gap are greater than 2,300), this explains the noticeable growth in the output flux at 8 L/min circulation rate compared to other circulation flow rates. Fig. 5b depicts the percentage increase in the permeate flux when the gap water is circulated compared to the permeate flux obtained with the conventional water gap system to visualize the flux enhancement. It is found that when the circulation is

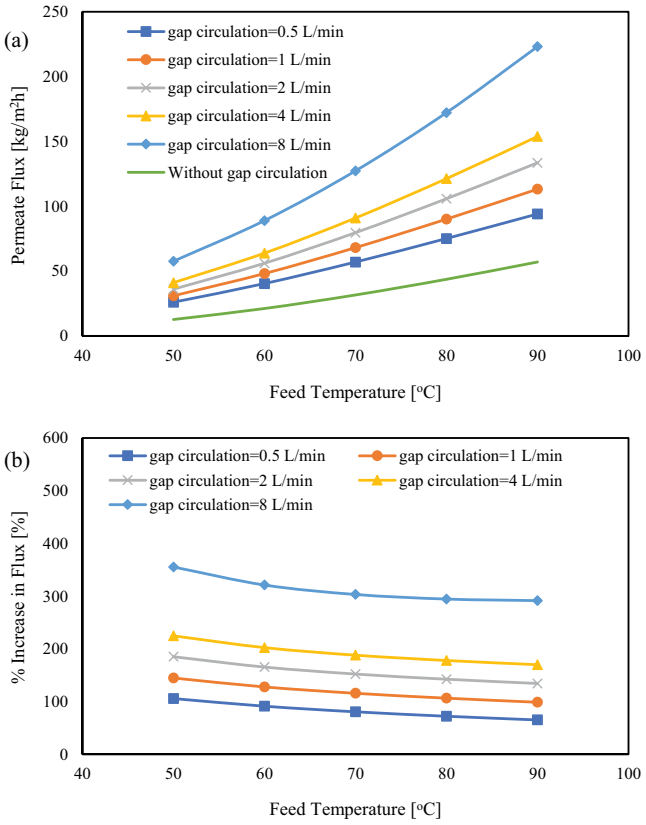

Fig. 5. Influence of flow circulation in the gap on output flux at various feed temperatures. Conditions: 15°C coolant temperature, 3 L/min cold and hot water flow rates, and 8 mm gap thickness.

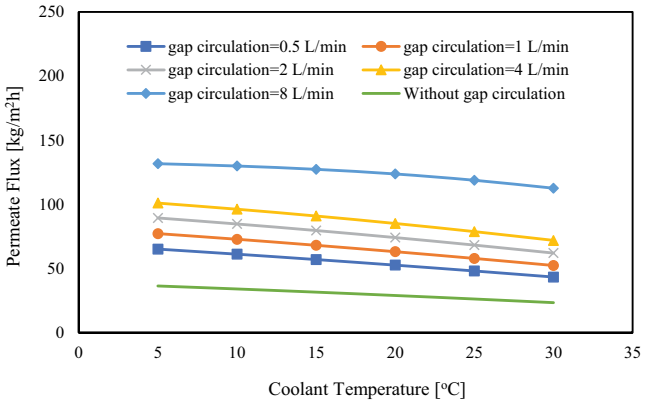

Fig. 6. Influence of circulated gap on output flux at various cold water temperatures. Conditions: 70°C feed temperature, 3 L/min cold and hot water flow rates, and 8 mm gap size.

used, the output flux increases by a maximum of about 355% at 50°C hot water temperature and 8 L/min gap flow rate. It can be noticed that at lower feed temperatures, the improvement in the permeate flux is more significant as a percentage. Therefore, adopting the flow circulation may be advantageous when the maximum hot water temperature is limited. At 90°C hot water temperature and 8 L/min circulation rate, flux increased by order of magnitude to roughly 220 kg/m²·h.

Another critical operating parameter of the MD system is the coolant temperature, as the permeation rate is directly related to the temperature variation between the heated and cooled membrane surfaces. In addition, the cooling stream is necessary to cool the gap water and maintain it at the required temperature. For the WGMD system, the thermophysical characteristics of the gap water are critical when modeling the overall mass and heat transfer. Therefore, it is believed that the gap water movement will improve heat transfer between the cold and hot streams, resulting in permeate flux enhancement.

The change in the flux with the temperature of the cold water is investigated, with and without circulation, as displayed in Fig. 6. The temperature of the cold stream is varied between 5°C and 30°C in 5°C increments. The feed temperature is 70°C for all coolant temperatures, the cold and hot water flow rates are 3 L/min, and the gap size is 8 mm.

Results indicate that reduced coolant temperature positively affects output flux for both systems due to the increased temperature variation through the membrane. When the cold water temperature is lowered from 30°C to 5°C, under the above-mentioned operating conditions, flux increases by a maximum of around 50% with a circulation flow rate of 0.5 L/min. However, within the same coolant temperature range, a roughly 55% improvement in permeate flux is observed for systems without circulation. This demonstrates that the coolant stream is more effective at cooling stagnant water than the circulating stream. It can be concluded that flow circulation in the gap increases the flux by a maximum of about 350% compared to a stagnant water gap, which is achieved at a coolant temperature of 30°C and a circulation flow rate of 8 L/min. It can be observed that at 8 L/min circulation flow rate the change in the flux associated with changing the coolant temperature is low compared to other flow values. Because at 8 L/min the flow rate inside the water gap is turbulent for all values of the cold water temperature, which makes the output flux less dependent on the variation of the coolant temperature.

Fig. 7 illustrates the influence of adjusting the hot water flow rate on the flux for both systems. With a gap thickness of 8 mm, hot and cold water temperatures of 70°C and 15°C, respectively, and a coolant flow rate of 3 L/min, the hot water flow rate is changed between 1 and 10 L/min to investigate the effect of hot water flow rate on output flux. In general, the output flux improves with rising the flow rate of the feed stream due to the enhancement of the turbulence level in the hot water flow channels resulting in improved mixing in the boundary layer and improved characteristics of heat transfer on the feed side of the membrane. Looking at Fig. 7, it can be noticed that when the hot water flow rate exceeds 3 L/min, the output flux abruptly rises due to the flow transformation from laminar to turbulent for Reynolds values more than 2,300. When the hot water flow rate is changed from 1 to 10 L/min, a considerable rise in permeate flux occurs, which is about 40% to 90% for the circulation flow rates of 0.5 to 4 L/min; however, the enhancement in flux with hot water flow rate is about 270% at a circulation flow rate of 8 L/min with a Reynold number of 2,700. In other words, the 270% increase of flux

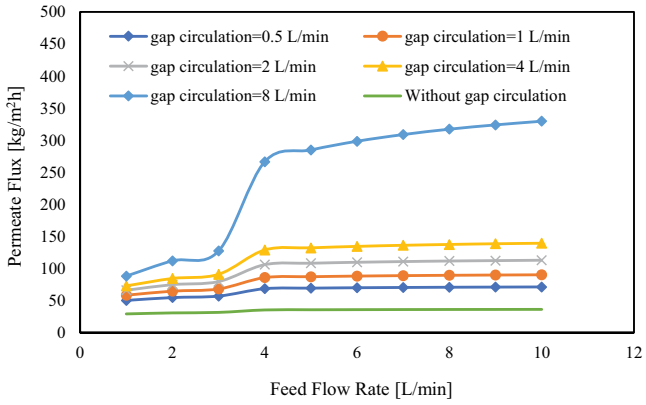

Fig. 7. Influence of circulation rate on output flux at various feed flow rates. Conditions: 70°C feed temperature, 15°C cold water temperature, 3 L/min cold water flow rate, and gap size of 8 mm.

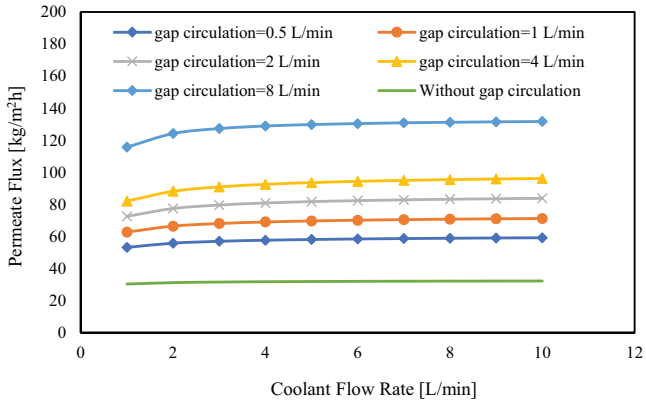

Fig. 8. Influence of flow circulation in the gap on output flux at various cold water flow rates. Conditions: 70°C feed temperature, 15°C coolant temperature, 3 L/min hot water flow rate, and 8 mm gap size.

at a hot water flow rate of 4 L/min and circulation rate of 8 L/min is the result of turbulent flow in both feed and gap channels which indicates the effect of forced heat transfer convection on the increase of the system's flux. The comparable increase in flux for a water gap without circulation is 25%, indicating that circulated gap functions better with a higher hot water flow rate, resulting in higher output flux values. From these percentages, it can be concluded that having a higher feed flow rate as well as a higher circulation flow rate is the optimum condition to obtain the maximum output flux of the WGMD system. At 10 L/min hot water flow rate and circulation flow rate of 8 L/min, the maximum output flux is achieved, which is about 330 kg/m²h.

To investigate its effect on the output flux, the cold water flow rate is changed within the same range as the hot water flow rate, while the other parameters remain constant at 70°C hot water temperature, 15°C cold water temperature, 3 L/min hot water flow rate, and 8 mm gap size. Fig. 8 illustrates the variance in output flux as a function of coolant flow rate for both systems. When the cold water flow rate is changed from 1 to 10 L/min, the permeate flux increases by an average of 14% for the system with circulation; however, it improves by about 6% for the system without circulation. The Reynolds number through the coolant channels varies between 225 (at a low flow rate of 1 L/min) and 2,250 (at a high flow rate of 10 L/min), remaining within the laminar flow region, which explains the gradual change in output flux as the cold water flow rate is increased. Along with the improvement produced by raising the cold water flow rate, the addition of the circulation results in further flux enhancement. The circulated gap water enhances permeate flux by a maximum of 300% compared to a system with a stagnant water gap, which is obtained at a circulation flow rate of 8 L/min.

When analyzing the performance of the WGMD unit, one of the most critical factors to be considered is the gap size. The MD process uses the gap to reduce heat loss between the cold and hot streams and thus the process's energy consumption. As a result, the gap size directly affects both the energy consumed and the output flux. The effect of flow circulation in the gap at various gap sizes is demonstrated in Fig. 9. In this case, the gap size is varied

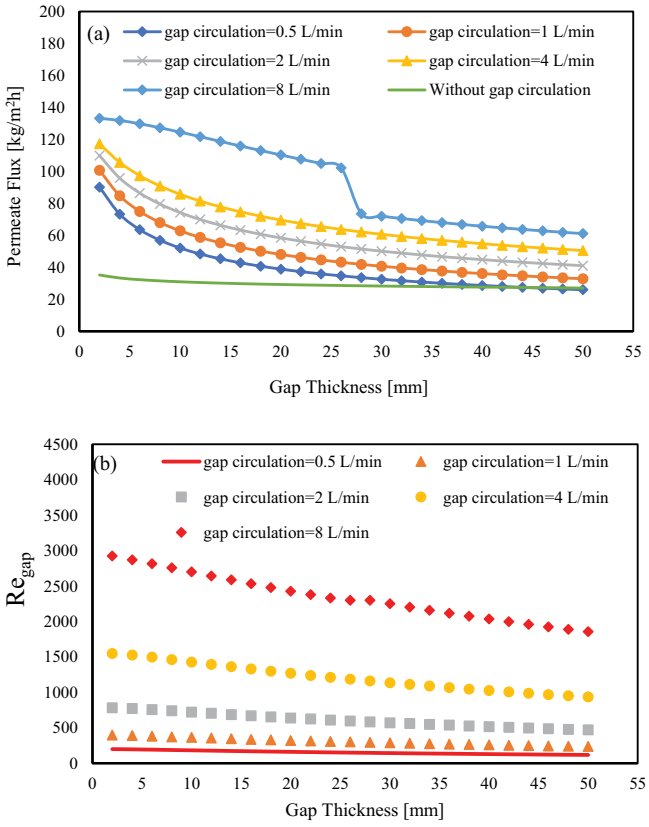

Fig. 9. Effects of gap thickness on flux and gap Reynolds number at different circulation rates. Conditions: 70°C hot water temperature, 15°C cold water temperature, 3 L/min cold and hot water flow rates.

between 2 and 50 mm. The analysis is conducted at constant operating temperatures of 70°C and 15°C for the feed and coolant, respectively, at flow rates of 3 L/min for the coolant and feed. As shown in Fig. 9, the output flux decreases noticeably as the gap size increases. changing the gap size from 2 to 50 mm reduces the output flux by a maximum of 71% at a circulation flow rate of 0.5 L/min. On the other

hand, there is only a 20% reduction in the flux observed when the gap size is changed from 2 to 50 mm for the system without circulation. Compared to the impact of feed and coolant temperatures, these lower percentages indicate that gap size has little effect on the output flux of WGMD system. This conclusion can be extremely beneficial in the design of improved MD systems, as it allows for a larger gap without negatively impacting system flux while providing additional space for internal design and manufacturing of circulation inlet and exit. It can be seen that at a higher circulation flow rate (8 L/min) there is a slight drop in the flux values with expanding the gap size up to 26 mm, then a significant decrease in the flux is obtained when the gap size is adjusted to 28 mm. This sudden drop is due to the transformation of the flow type inside the gap from turbulent to laminar at a gap thickness of 28 mm, which can be observed from the values of Reynolds number within the water gap as shown in Fig. 9b. Fig. 9b also represents the variation for gap flow rates from 0.5 to 4 l/min showing a laminar flow for all cases. This is the main reason behind the absence of a sudden drop in the stated flow rates in Fig. 9a.

The variations of the channel Reynolds number (Re) heat transfer coefficient in both the feed channel (*h-f*) and gap circulation channels (*h*-gap) are presented collectively in Fig. 10, for different feed and circulation flow rates. The flow rates of the feed water and the circulation gap water are changed from 1 to 8 L/min. Data analysis reveals a

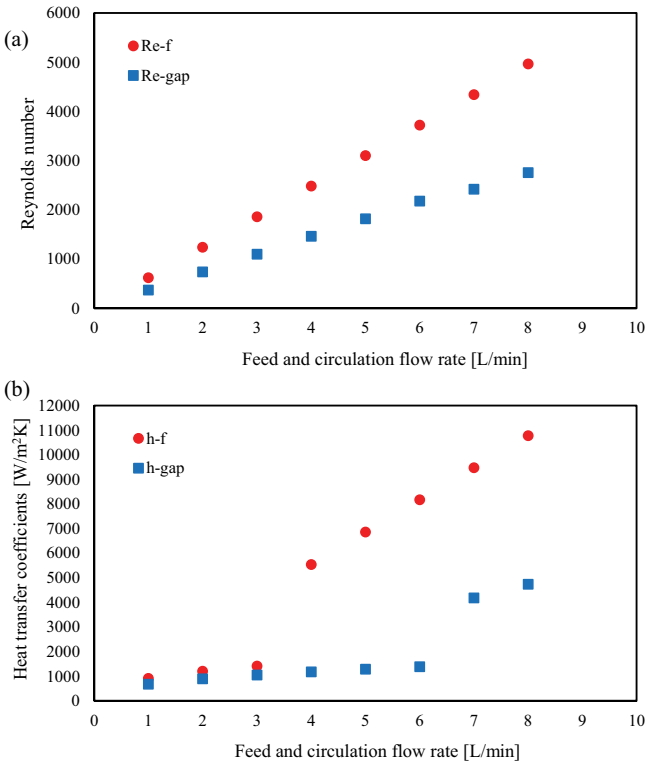

Fig. 10. Effects of feed and gap flow rates on the heat transfer coefficient and Reynolds number. Conditions: 70°C hot water temperature, 15°C cold water temperature, 3 L/min cold water flow rate, and 8 mm gap thickness.

relationship between the flow characteristics (as identified by the channel Reynolds number) and the heat transfer coefficient. At a given flow rate, the channel Reynolds number in the feed channel is higher than that in the gap channel due to the higher feed stream temperature. In general, as the flow rate increases, the Reynolds number increases until reaching the transition from laminar to turbulent flow (at Re = 2,300) where the a notable rise in the heat transfer coefficient is commenced in both the feed and gap channel flows. This is the reason behind the abruptly change if flux presented before in Figs. 4b, 7, and 9a. the flow transition takes place at a flow rate between 3 and 4 L/min in the hot feed channel, while the corresponding transition in the gap channel occurs between 6 and 7 L/min. It is worth mentioning that the Reynolds number (and flow transition) depends on the flow rate, channel geometry & dimensions, and fluid properties which are mainly functions of fluid temperature.

4.2. Energy performance

Many variables influence the SEC and GOR of the WGMD unit; however, the hot water temperature is the most significant factor. The following analysis examines the impact of circulation on the GOR and SEC at various hot water temperatures and circulation flow rates. This analysis is carried out under constant operating conditions of 15°C coolant temperature, 3 L/min cold and hot water flow rates, and a gap size of 8 mm. Fig. 11 compares SEC and GOR of the water gap system with and without circulated gap. Results reveal that the circulated gap system shows better energy performance (higher GOR and less SEC), compared to non-circulated gap system, for the circulation rates up to 4 L/min. When the circulation flow rate rises to 8 L/min, the module with circulation has lower energy performance (lower GOR and higher SEC) than a module with no circulation. This decrease in energy efficiency results from the increased energy loss between the cold and hot streams caused by the increased circulation rate. Compared to the enhancement in the production rate that is obtained at a circulation rate of 8 L/min, the reduction in energy efficiency is marginal. For example, when a circulation flow rate of 8 L/min is used, the permeate flux increases by an average of about 300% compared to that for the system with no circulation; however, the GOR decreases by approximately 20%, and the SEC increases by approximately 24% on average.

The circulation flow rate affects both the permeate flux and energy consumption by influencing the temperature profile through the MD module. To study the impact of circulation flow rate on the temperature profile in the WGMD module, the feed and coolant temperatures are held constant at 70°C and 15°C, respectively, while different flow rate are used. As shown in Fig. 12, as the flow rate increases, both the membrane temperature and the gap temperature decrease, indicating that higher flow rates enhance the cooling efficiency of the module. This is a favorable outcome as lower membrane temperature values promote the efficient separation of water vapor from the feedwater, a fundamental objective in membrane distillation. However, it can be noticed that the cooling plate temperature rises with increasing flow rates, indicating that the cooling plate and cooling stream may be absorbing more heat as the gap water passes

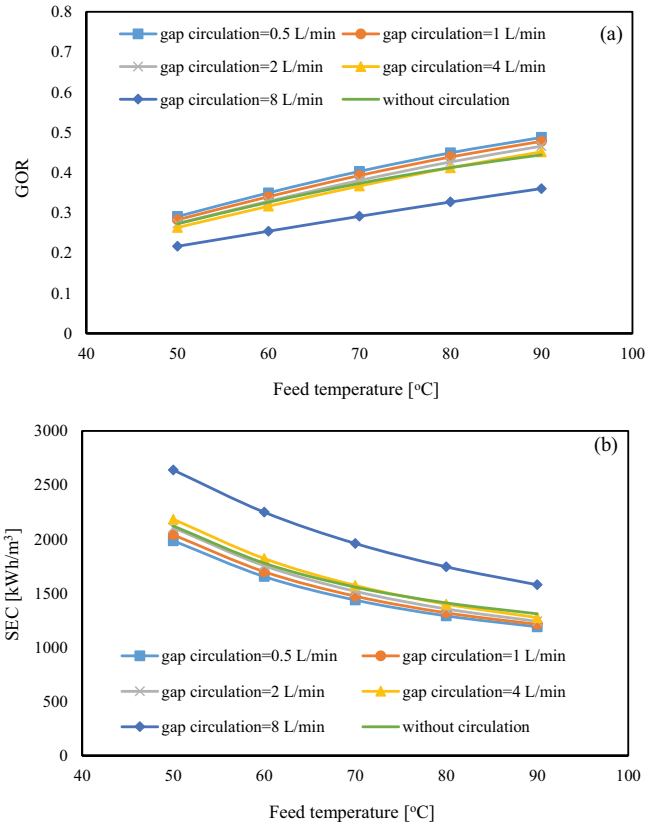

Fig. 11. Influence of hot water temperature and circulation rate on the system GOR and SEC. Conditions: 15°C cold water temperature, 3 L/min cold and hot water flow rates, and gap size of 8 mm.

through the module more rapidly. The interplay of these temperature changes underlines the balance required for optimal membrane distillation performance, where efficient cooling is essential for vapor transport through the membrane while managing the cooling stream temperature to maintain overall system stability and efficiency.

4.3. Cost estimation

The work of Al-Obaidani et al. [22] was used to develop the following model, which estimates the cost of producing freshwater using the proposed system. The cost model includes both operating and maintenance costs (OMC) and capital costs (CC). The assumptions made in the cost modeling [22–25]: life of the MD system (n) = 20 y, system/plant availability (Ƒ) = 90%, interest rate (i) = 5%, specific membrane cost (SMC) = \$90 m^{-2}, specific electricity cost (SEC) = \$0.03 kWh, specific membrane replacement cost (SMRC) = 0.15 (15%/y), specific labor cost (SLC) = \$0.03 m^{-3}, specific spare parts cost (SSC) = \$0.033 m^{-3}, specific chemicals cost (SCC) = \$0.018 m^{-3}, specific steam cost (SSC) = \$0.007/kg, specific brine disposal cost (SBDC) = \$0.0015 m^{-3}, steam heat exchanger cost (SSHXC) = \$2000 m^{-2}, pressure drop in the feed side (ΔP_{drop_f}) = 1.01325 × 10^5 Pa and pressure drop in the coolant side (ΔP_{drop_c}) = 1.01325 × 10^5 Pa. The specific cost of civil work and cost of intake and pretreatment are

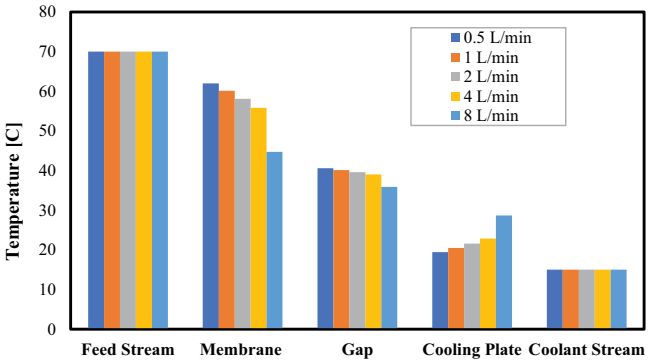

Fig. 12. Influence of circulation rate on the temperature distribution inside the MD module. Conditions: 70°C hot water temperature, 15°C cold water temperature, 3 L/min cold and hot water flow rates, and gap size of 8 mm.

neglected [26]. The expressions for the freshwater cost estimation [22]:

4.3.1. For the direct capital costs (DCC)

$$\text{Feed pumps cost}\left(\text{FPC}\right) = 4.78\times10^{-6}\left(\frac{P_{\text{MD}}}{\text{RR}}\right)\Delta P_{\text{drop}_f} \tag{22}$$

$$\text{Coolant pumps cost}\left(\text{CPC}\right) = 4.78\times10^{-6}\left(\frac{P_{\text{MD}}}{\text{RR}}\right)\Delta P_{\text{drop}_c} \tag{23}$$

where P_{MD} is the system production rate in m^3/d, RR is the recovery ratio.

$$\text{Membrane cost}\left(\text{MC}\right) = \text{MA}\times\text{SMC} \tag{24}$$

where MA is the membrane area.

$$\text{Heat exchanger area}\left(\text{HXA}\right) = \frac{E_{\text{iin}}}{U\times T_{\text{av}}} \tag{25}$$

where $E_{\text{iin}} = \dot{m}_f \times \text{Cp}_f \times \left(T_{f,\text{in}} - T_{f,\text{out}}\right)$

where U = 2,500 W/m^2 °C = U: global heat transfer coefficient.

$$\text{Cost}\left(\$\right)\text{ of heat exchangers}\left(\text{HXC}\right) = \text{HXA}\times\text{SSHXC} \tag{26}$$

$$\text{Direct capital costs}\left(\text{DCC}\right) = \text{FPC} + \text{CPC} + \text{MC} + \text{HXC} \tag{27}$$

4.3.2. For the indirect capital cost (ICC)

$$\text{ICC} = \text{DCC}\times 0.1 \tag{28}$$

$$\text{Capital cost}\left(\text{CC}\right) = \text{ICC} + \text{DCC} \tag{29}$$

$$\text{Annual Capital Cost}\left(\text{ACC}\right)\left(\$/\text{m}^3\right) = \alpha\times\text{CC}/\left(Ƒ\times P_{\text{MD}}\times 365\right) \tag{30}$$

$$\text{Where amortization factor } (\alpha) = \frac{i(i+1)^n}{(i+1)^n - 1} \quad (31)$$

4.3.3. Maintenance and operational costs (MOC)

$$\text{Membrane replacement cost } (\text{OMRC}) = \text{SMRC} \times \text{MC} \quad (32)$$

$$\text{Electricity cost } (\text{COE}) = \text{SEC} \times \text{SEEC} \times (\text{ℱ} \times P_{\text{MD}} \times 365) \text{ for the pumps} \quad (33)$$

where $\text{SEEC} = \frac{F_{\text{feed}} \times \Delta P_{\text{drop}}}{365 \times \eta_{\text{pump}} \times F_{\text{dist}}}$, F_{feed} = water circulation rate (L/h), F_{dist} distillate production rate (L/h), ΔP_{drop} = hydraulic pressure drop in WGMD module (bar), and η_{pump} = 0.85 = efficiency of the water-circulating pump.

$$\text{Cost } (\$/\text{y}) \text{ of steam } (\text{COSS}) = \text{SSC} \times \dot{m}_{\text{steam}} \times (60 \times 60 \times 24 \times 365) \times \text{ℱ} \quad (34)$$

$$\text{Chemicals cost } (\text{COC}) = \text{SCC} \times (\text{ℱ} \times C_{\text{MD}} \times 365) \quad (35)$$

$$\text{Spare parts cost } (\text{COSP}) = \text{SSC} \times (\text{ℱ} \times P_{\text{MD}} \times 365) \quad (36)$$

$$\text{Labor cost } (\text{COL}) = \text{SCL} \times (\text{ℱ} \times P_{\text{MD}} \times 365) \quad (37)$$

$$\text{Brine disposal cost } (\text{COBD}) = (\text{ℱ} \times P_{\text{MD}} \times 365) \times \text{SCBD} \quad (38)$$

$$\text{Total annual } M \,\&\, O \text{ cost } (\$/\text{year}) = \text{COSP} + \text{COMR} + \text{COBD} + \text{COE} + \text{COSS} + \text{COC} + \text{COL} \quad (39)$$

$$\text{Annual } M \,\&\, O \text{ Cost } (\$/\text{m}^3) = \text{Total annual } M \,\&\, O \text{ cost}/(\text{ℱ} \times P_{\text{MD}} \times 365) \quad (40)$$

$$\text{Freshwater cost} (\$/\text{m}^3) = \text{Annual } O \,\&\, M \text{ Cost} + \text{Annual Capital Cost} \quad (41)$$

Similar to energy analysis, the feed temperature is used to examine the effect of the circulation on the cost. Fig. 13 shows the impact of circulation on the production cost at various hot water temperatures. For both designs, with and without circulation, a significant drop in the cost occurs when increasing the hot water temperature; however, this reduction is less than the change observed in the output flux when the hot water temperature is changed because rising the feed temperature consumes more energy; therefore, the cost of energy increases as well. For example, shifting the hot water temperature from 50°C to 90°C leads to almost 270% and 350% enhancement in the permeate flux for the WGMD system with and without circulation, respectively. On the other hand, only 46% (on average) and 60% reduction in the cost is achieved when the temperature of the feed is changed within the same range. The cost is inversely linked to the system's permeate flux; the cost is low for higher values of the output flux. As a result, circulation significantly reduces the cost compared to the same design without circulation. When the gap water is circulated, the production cost reduces by an average of 25%–32%, for different circulation rates, compared to the conventional water gap design.

From Fig. 13, it is observed that the production cost of the WGMD systems is inversely related to the system's permeate flux; the cost is low for higher values of the output flux. For further investigation, the variation of the cost with the productivity is presented, as shown in Fig. 14. The productivity of the MD process can be enhanced by scaling up the system or using a multistage arrangement. To study the variation of the cost with the system productivity, it is assumed that multiple MD units, which are connected in parallel, are used. It is observed that using a multistage system results in improving the system's productivity. A significant decrease in the cost is achieved when the production rate increases from 10 to 60 L/d (about 60%). However, increasing the production rate above 50 L/d up to 195 L/d leads to a slight decrease in the cost (about 18%) due to the increase in the capital and operating cost of the multistage system.

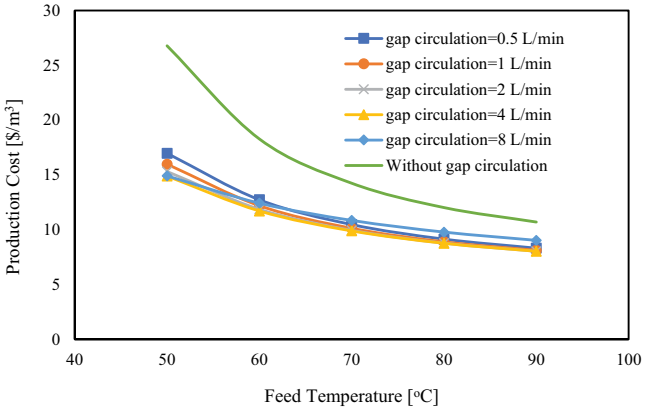

Fig. 13. Influence of flow circulation in the gap on production cost at various feed temperatures. Conditions: 25°C cold water temperature, 3 L/min cold and hot water flow rates, and 8 mm gap size.

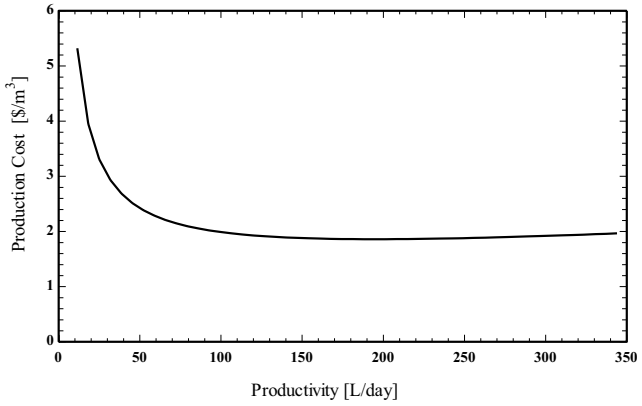

Fig. 14. Influence of the production rate on production cost. Conditions: 70°C hot water temperature, 25°C cold water temperature, 3 L/min cold and hot water flow rates, 2 L/min circulation flow rate, and 8 mm gap size.

To raise the production rate to more than 195 L/d about 17 stages are needed to be employed, which significantly increases the capital and operating cost of the system. For this reason, a slight jump in the cost values is obtained when the production rate is more than 195 L/d. The lowest value of the cost is achieved at 195 L/d, which is about 1.8 $/m^3. Enhancing productivity by using a multistage system can reduce the production cost by about 82% (from 10 $/m^3 for the single-stage system to 1.8 $/m^3 for the multistage system).

5. Conclusions

The theoretical investigation of a novel design of the WGMD method is conducted to improve the productivity for the same operating conditions. The model considers both heat and mass transfer throughout the MD module. In this system, it is assumed that the freshwater inside the gap is constantly moving and circulating. The accuracy of the results is demonstrated by validating the built model compared to experimental findings of the same design. Then, the model is applied to study the impact of circulated gap on the system performance over a wide range of operating parameters. The operational variables include the temperatures and flow rates of both the cold and hot streams, the flow rate of the circulating water, and the size of the water gap. Performance indicators, on the other hand, include the SEC, output flux, freshwater production cost, and GOR. Furthermore, the effects of some cost components on the system production cost of both systems are investigated. Finally, the new model's performance is compared to the same-design conventional WGMD unit.

Results indicated that when the water in the gap is circulated, the output flux of the WGMD process dramatically increases. This improvement results from improved mixing in the distillate channel, which results in a uniform temperature distribution within the gap. Furthermore, water flow raises the heat and mass transfer coefficients in the gap, increasing the rate of condensation and consequently freshwater production. The circulated gap water significantly increases output flux, with a maximum increase of about 350% at hot water temperature of 50°C and a gap flow rate of 8 L/min.

It has been demonstrated that flux enhancement is associated with increased energy consumption, as indicated by temperature differences between the inlet and outlet of both the feed and coolant streams. As a result, a slight improvement in energy efficiency is obtained when the gap water is circulated at a rate up to 4 L/min. On the other hand, using a higher circulation flow rate of 8 L/min reduces the energy efficiency (reduces the GOR and increases the SEC) compared to the conventional one; however, the difference in energy efficiency between the two systems is only about 20% for the GOR and 24% for the SEC, which is very small relative to the increase in output flux achieved by using the circulation.

In terms of production cost, the system with circulation is capable of significantly lowering the cost. For example, around 25%–32% of the production cost is saved when circulating the gap water. Enhancing the system's productivity using a multistage system can reduce the production cost by about 82%.

The data provided within this research paper serves as a valuable resource for evaluating process performance, which is helpful in guiding future technological advancements and optimization efforts. These endeavors are essential as they are geared towards the development and commercialization of this technology on a larger scale.

Acknowledgment

The authors gratefully acknowledge the assistance and funding provided by the Interdisciplinary Research Center in Renewable Energy and Power Systems (IRC-REPS) at King Fahd University of Petroleum & Minerals through Research Grant # INRE2206.

References

[1] N.M.A. Omar, M.H.D. Othman, Z.S. Tai, A.O.A. Amhamed, T.A. Kurniawan, M.H. Puteh, M.N.M. Sokri, Recent progress, bottlenecks, improvement strategies and the way forward of membrane distillation technology for arsenic removal from water: a review, J. Water Process Eng., 52 (2023) 103504.
[2] S.M. Shalaby, A.E. Kabeel, H.F. Abosheiasha, M.K. Elfakharany, E. El-Bialy, A. Shama, R.D. Vidic, Membrane distillation driven by solar energy: a review, J. Cleaner Prod., 366 (2022) 132949, doi: 10.1016/j.jclepro.2022.132949.
[3] Z.S. Tai, M.H.D. Othman, K.N. Koo, J. Jaafar, Critical review on membrane designs for enhanced flux performance in membrane distillation, Desalination, 553 (2023) 116484, doi: 10.1016/j.desal.2023.116484.
[4] A.M. Alklaibi, N. Lior, Membrane-distillation desalination: status and potential, Desalination, 171 (2005) 111–131.
[5] A. Alkhudhiri, N. Darwish, N. Hilal, Membrane distillation: a comprehensive review, Desalination, 287 (2012) 2–18.
[6] F.A. Banat, J. Simandl, Desalination by membrane distillation: a parametric study, Sep. Sci. Technol., 33 (1998) 201–226.
[7] A.E. Khalifa, Water and air gap membrane distillation for water desalination – an experimental comparative study, Sep. Purif. Technol., 141 (2015) 276–284.
[8] M.A. Abu-Zeid, Comparison of the effect of air and permeate gap regions on highly saline water desalination using hollow fiber membrane distillation modules, J. Soil Sci. Agric. Eng., 12 (2021) 417–424.
[9] J. Cai, H. Yin, F. Guo, Transport analysis of material gap membrane distillation desalination processes, Desalination, 481 (2020) 114361, doi: 10.1016/j.desal.2020.114361.
[10] M. Essalhi, M. Khayet, Application of a porous composite hydrophobic/hydrophilic membrane in desalination by air gap and liquid gap membrane distillation: a comparative study, Sep. Purif. Technol., 133 (2014) 176–186.
[11] L. Francis, N. Ghaffour, A.A. Alsaadi, G.L. Amy, Material gap membrane distillation: a new design for water vapor flux enhancement, J. Membr. Sci., 448 (2013) 240–247.
[12] A.E. Khalifa, Flux enhanced water gap membrane distillation process-circulation of gap water, Sep. Purif. Technol., 231 (2020) 115938, doi: 10.1016/j.seppur.2019.115938.
[13] S.M. Alawad, D.U. Lawal, A.E. Khalifa, I.H. Aljundi, M.A. Antar, T.N. Baroud, Analysis of water gap membrane distillation process with an internal gap circulation propeller, Desalination, 551 (2023) 116379, doi: 10.1016/j.desal.2023.116379.
[14] S.M. Alawad, D.U. Lawal, A.E. Khalifa, I.H. Aljundi, M.A. Antar, T.N. Baroud, M.A. Mohammed Eltoum, Optimization and design analysis of multistage water gap membrane distillation for cost-effective desalination, Desalination, 566 (2023) 116894, doi: 10.1016/j.desal.2023.116894.
[15] F. Mahmoudi, G.M. Goodarzi, S. Dehghani, A. Akbarzadeh, Experimental and theoretical study of a lab scale permeate gap membrane distillation setup for desalination, Desalination, 419 (2017) 197–210.

[16] M. Khayet, T. Matsuura, Membrane Distillation: Principles and Applications, Elsevier, Amsterdam, The Netherlands, 2011.
[17] T.-C. Chen, C.-D. Ho, H.-M. Yeh, Theoretical modeling and experimental analysis of direct contact membrane distillation, J. Membr. Sci., 330 (2009) 279–287.
[18] M. Khayet, Membranes and theoretical modeling of membrane distillation: a review, Adv. Colloid Interface Sci., 164 (2011) 56–88.
[19] S.M. Alawad, A.E. Khalifa, Analysis of water gap membrane distillation process for water desalination, Desalination, 470 (2019) 114088, doi: 10.1016/j.desal.2019.114088.
[20] B.-G. Im, J.-G. Lee, Y.-D. Kim, W.-S. Kim, Theoretical modeling and simulation of AGMD and LGMD desalination processes using a composite membrane, J. Membr. Sci., 565 (2018) 14–24.
[21] A. Ruiz-Aguirre, J.A. Andrés-Mañas, J.M. Fernández-Sevilla, G. Zaragoza, Experimental characterization and optimization of multi-channel spiral wound air gap membrane distillation modules for seawater desalination, Sep. Purif. Technol., 205 (2018) 212–222.
[22] S. Al-Obaidani, E. Curcio, F. Macedonio, G. Di Profio, H. Al-Hinai, E. Drioli, Potential of membrane distillation in seawater desalination: thermal efficiency, sensitivity study and cost estimation, J. Membr. Sci., 323 (2008) 85–98.
[23] A.M. Helal, A.M. El-Nashar, E. Al-Katheeri, S. Al-Malek, Optimal design of hybrid RO/MSF desalination plants Part I: modeling and algorithms, Desalination, 154 (2003) 43–66.
[24] A. Malek, M.N.A. Hawlader, J.C. Ho, Design and economics of RO seawater desalination, Desalination, 105 (1996) 245–261.
[25] F. Macedonio, E. Curcio, E. Drioli, Integrated membrane systems for seawater desalination: energetic and exergetic analysis, economic evaluation, experimental study, Desalination, 203 (2007) 260–276.
[26] A.E. Kabeel, T.A. Elmaaty, E.M.S. El-Said, Economic analysis of a small-scale hybrid air HDH–SSF (humidification and dehumidification–water flashing evaporation) desalination plant, Energy, 53 (2013) 306–311.